CREEP BEHAVIOR OF AN EASY ORIENTED Ti-48Al PST CRYSTAL①

Lin Jianguo, Zhou Yajian, Zhang Yonggang, Chen Changqi
Department of Materials Science and Engineering,
Beijing University of Aeronautics and Austronautics, Beijing 100083

ABSTRACT The creep deformation behavior of an easy oriented PST crystal was investigated at 800 ℃ in compression creep. The stress range was 120 MPa to 200 MPa. The creep curves showed a steady state stage. The application of a power-law equation led to a stress exponent $n = 6.6$ and the creep activation energy $Q_c =$ 282 kJ/mol, which indicated that dislocation climb controlls creep mechanism. TEM observation of the crept samples at steady state regime showed the formation of substructures in some γ plates.

Key words TiAl alloy PST crystal creep behavior

1 INTRODUCTION

Among intermetallic alloys under development for high temperature structural applications, γ-TiAl-base alloys have been, and continue to be, the most attractive one to the aerospace industry due to their low density, high strength retention at elevated temperatures. Because of the brittleness of these alloys at temperature below ~ 700 ℃, most of the research activities has focused essentially on the optimization of room temperature ductility and fracture toughness via suitable alloying additions and microstructure control[1-3]. Because Creep property of γ-TiAl alloys is important to its use as a potential high temperature materials, without a fundamental understanding of creep behavior, there is greater risk associated with the use of γ-TiAl in the envisaged critical propulsion applications. So far, the work on creep behavior of γ-TiAl has been limited to the polycrystalline alloys due to their complication of the microstructure[4-6], therefore, little knowledge and understanding in creep behavior of the alloys has been gained.

Yamaguchi *et al*[7] have succeed in growing the so-called polysynthetically twinned (PST) crystals of TiAl, which contains only a single grain with two phases TiAl/Ti_3Al lamellar structure, providing a good simulating material for studying the deformation mechanism in two phases alloys with fully lamellar structure. Studies on the tensile or compression properties of PST crystals indicated that the deformation mechanism of PST crystals strongly depend on the angle φ between the lamellar boundaries and the loading axis, and there exist two types of deformation depending on the angle φ. When the φ = 0° or 90°, shear deformation occurs across the boundaries and yield strength is high, which is called the hard-type deformation; when the angle φ varies from 35° to 75°, the yield strength is low, which is called the easy-type deformation.

In present study, Ti-48Al PST crystals were prepared by using induction floating zone melting furnace, and the creep behavior of specimens oriented with easy-type deformation was investigated. The purpose is attempt to detect the creep mechanism of lamellar structure with this orientation.

2 EXPERIMENTAL

The master ingot with nominal composition of Ti-48Al was prepared by induction levitation melting Ti sponge and high purity Al in a water

① Received Jan. 26, 1996; accepted Jun. 18, 1996

cooled copper crucible. Rods, 8 mm in diameter and 100 mm long, were cut from the master ingot. The PST crystals were grown from the rods using an induction floating zone melting furnace by controlling the growth rate under an argon atmosphere. Compression samples, approximately 3 mm × 3 mm in cross section and 5.5 mm long, were cut from as-grown crystals with the traces of the lamellar boundaries perpendicular to the compressive axis on the X-face, while on Y-face the lamellar boundaries were seen to edge on, as shown in Fig. 1. The angle between lamellar boundary and compressive axis was represented by φ, which was 45° in the samples.

Compression creep testing was conducted at 850 ℃ in air under constant load control on a compression creep test machine equipped with lever arms of 10∶1. The stress level ranges from 120 MPa to 200 MPa. An optical measurement system was used to monitor and record strain data. Minimum creep rates were determined using sliding regression.

The deformation structure of the crept samples were preserved by cooling the samples under load. The TEM foils were prepared by jet using an electrolytic solution of 8% (in volume) perchloric acid + alcohol. TEM investigations were conducted on Hitachi H-800 operating at 150 kV with double tilt stage.

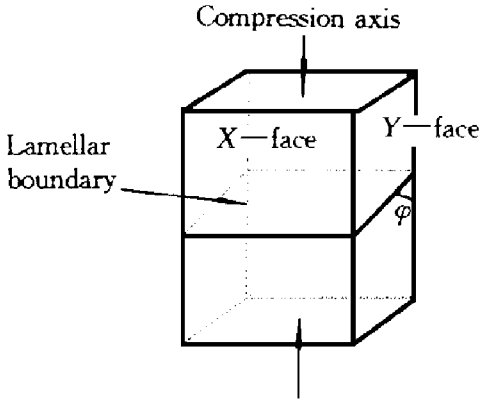

Fig. 1 Geometry of compression specimen

3 RESULTS

3.1 Determination of the crystallographic orientation of the loading axis

The orientation relationship between the TiAl and Ti_3Al phases in the lamellar structure of Ti-rich TiAl compounds has been reported in detail in the previous paper[7], i.e. $(111)_\gamma \parallel (0001)_{\alpha_2}$ and $[1\bar{1}0]_\gamma \parallel \langle 11\bar{2}0\rangle_{\alpha_2}$. Since three $\langle 11\bar{2}0\rangle$ directions on the basal plane in the Ti_3Al phase with the hexagonal $D0_{19}$ structure are all equivalent while the $[1\bar{1}0]$ direction and the other two $\langle 10\bar{1}]$ and $\langle 01\bar{1}]$ directions on the (111) plane in the TiAl phase with tetragonal $L1_0$ structure are not equivalent to each other, there are six possible orientations of the $[1\bar{1}0]$ directions in the TiAl phase with respect to $\langle 11\bar{2}0\rangle$ directions in the Ti_3Al phase, that is

$$\begin{aligned}
&[\mathrm{I}][1\bar{1}0]_\gamma \uparrow\uparrow [11\bar{2}0]_{\alpha_2},\\
&[\mathrm{II}][1\bar{1}0]_\gamma \uparrow\uparrow [\bar{1}20]_{\alpha_2},\\
&[\mathrm{III}][1\bar{1}0]_\gamma \uparrow\uparrow [\bar{2}110]_{\alpha_2} \qquad (1)\\
&[\mathrm{I}][1\bar{1}0]_\gamma \downarrow\uparrow [11\bar{2}0]_{\alpha_2},\\
&[\mathrm{II}][1\bar{1}0]_\gamma \downarrow\uparrow [\bar{1}20]_{\alpha_2},\\
&[\mathrm{III}][1\bar{1}0]_\gamma \downarrow\uparrow [\bar{2}110]_{\alpha_2} \qquad (2)
\end{aligned}$$

where $\uparrow\uparrow$ and $\downarrow\uparrow$ mean parallel and antiparallel. Thus, in the TiAl/Ti_3Al lamellar structure, the TiAl phase can exist in six orientation variants. The TiAl domains with six variants can be classified into two types of domains, i.e., the matrix domains corresponding to the variants [I], [II] and [III] in Eqn. (1), and twin domains corresponding to the variants [I], [II] and [III] in Eqn. (2). The thin foil was cut parallel to the Y-face of the crept samples, and its normal was determined nearly to be $\langle 1\bar{1}0\rangle$. Thus, the orientation of loading axis with respect to the matrix domains of the variant [I] was calculated to be $[44\bar{1}]$.

3.2 Creep behavior

The creep curves of the samples with $\varphi = 45°$ at different stress levels are shown in Fig. 2, as strain vs. time (ε-t) plots.

The creep curves are essentially of normal type. After the initial strain on loading, the creep rate decreases gradually during "primary stage", until an apparently constant or steady-state rate is reached during the "secondary stage". The extent of the three stages can vary

markedly with respect to strain and time for different stress conditions. With the increase of stress level, the duration of the steady-state stage became short, or disappeared, and the tertiary stage was onset early. The minimum creep rates for different stress levels measured through the linear regress method are listed in Table 1.

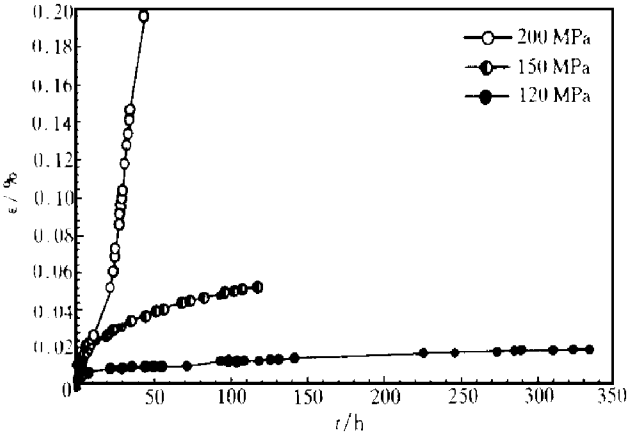

Fig. 2 Creep strain vs. time of the samples with $\varphi = 45°$ at 800 ℃

Table 1 Minimum creep rate at different stress levels

Orientation /(°)	Stress level /MPa	Temperature / ℃	Minimum creep rate/ h^{-1}
45	120	800	3.31×10^{-5}
	150	800	2.39×10^{-4}
	200	800	1.49×10^{-3}

The stress dependence of the minimum creep rate is usually described by power law according to $\dot{\varepsilon}_m = A\sigma^n(Q_c/RT)$[8], where A is a constant, Q_c is the activation energy for creep, R the gas constant, T the absolute temperature, n the stress exponent.

This equation yields a linear relation between $\dot{\varepsilon}_m$ and σ in a double logarithmic plot. The slope of this curve yields a stress exponent n. The stress dependence of the minimum creep rate for specimens with $\varphi = 45°$ at 800 ℃ is shown in Fig. 3(a). It can be seen that well-defined linear relations are obtained, which demonstrates that the creep rates for PST crystals with $\varphi = 45°$ in the present experimental conditions exhibit a power law dependence on the applied stress. The value of stress exponents is equal to the slope of line, i.e. $n = 6.6$, which is slightly higher in comparison to the value found in *fcc* metals and alloys for dislocation creep.

The activation energy for the secondary creep was determined by deforming a series of specimens at the same stress but at different temperatures, e.g. 700 ℃, 750 ℃, 800 ℃, 850 ℃. According to the power law, Arrhenius type curve was plotted for $\ln\dot{\varepsilon}_m$ with reciprocal test temperature, $1/(RT)$, under stress of 150 MPa, as shown in Fig. 3(b), in which well-defined linear relations are also obtained. From the slope of the curve in Fig. 3(b), the activation energy for the secondary creep were determined, which was 282 kJ/mol, and quite close to the activation energy for self diffusion of Ti in single phase TiAl, i.e. 290 kJ/mol[9].

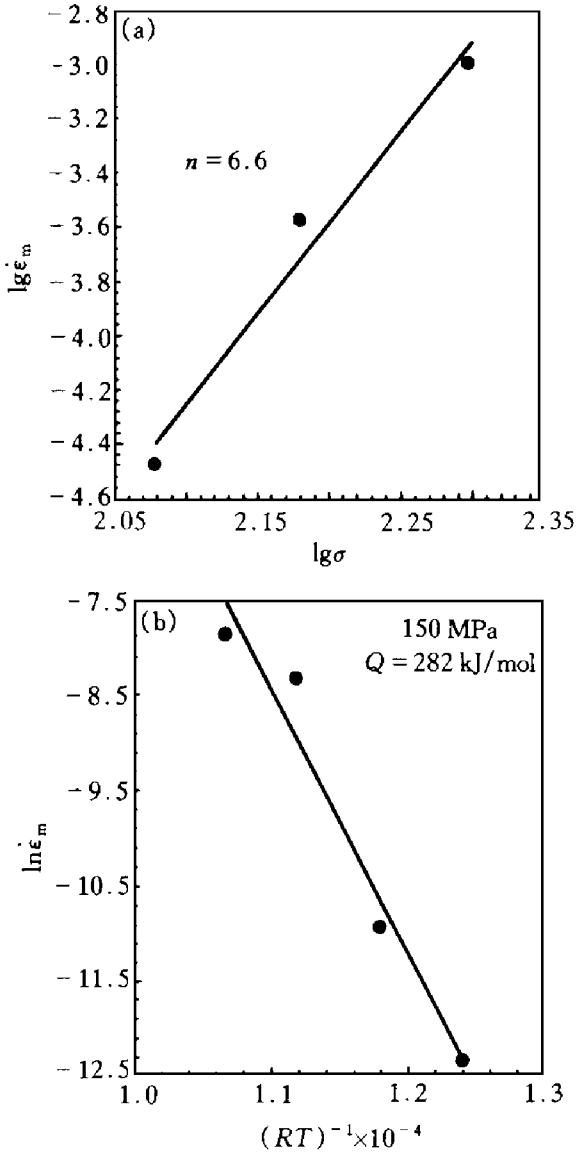

Fig. 3 Stress and temperature dependence of the minimum creep strain rate of the samples with $\varphi = 45°$

3.3 Deformed microstructure during secondary creep

Fig. 4 shows the micrographs of the deformed structure corresponding to the secondary creep regime of the specimens at 150 MPa. It can be seen that the deformation occurred primarily parallel to the lamellar boundaries, and no dislocations, or deformation twins were seen to pile up at the boundaries. The deformation microstructures in different γ plates are quite different, and dislocation tangles and substructures constitute the main deformation microstructures in most γ plates, as shown in Fig. 4(a). The dislocation walls and subgrains can be seen in many γ plates, as shown in Fig. 4(b), (c), which are thought to be formed as result of climb of edge segments. Deformation twins are occasionally found in some γ plates of the crept specimens, as shown in Fig. 4(d).

4 DISCUSSION

Six different types of ordered domain existing in TiAl phase constituting in TiAl/Ti_3Al lamellar structure have been established, and the crystallographic orientations of the loading axis with respect to the matrix domains of the variant I has also been determined. Thus, the Schimd factors for the slip systems and twinning on the (111) planes parallel to the boundaries in six types of TiAl domains can be calculated, which is listed in Table 2.

Because the angle between the lamellar boundaries and the loading axis is 45°, the slip or twinning systems with the highest Schmid factors are on the (111) planes parallel to the lamellar boundaries. So the shear deformation will occur along the lamellar boundaries, and the dislocations or twins will not interact with the boundaries, as seen in Fig. 4. Otherwise, the situation of the deformation in each γ plate is quite different. It depends on the magnitude of the Schmid factors for slip or twinning system. From Table 2, we can see that, in γ plates with variant I, $1/6[11\bar{2}]$ twinning system has the highest Schmid factor, so the activity of twinning is favor in these γ plates. While in other γ plates with varient II or varient III, the

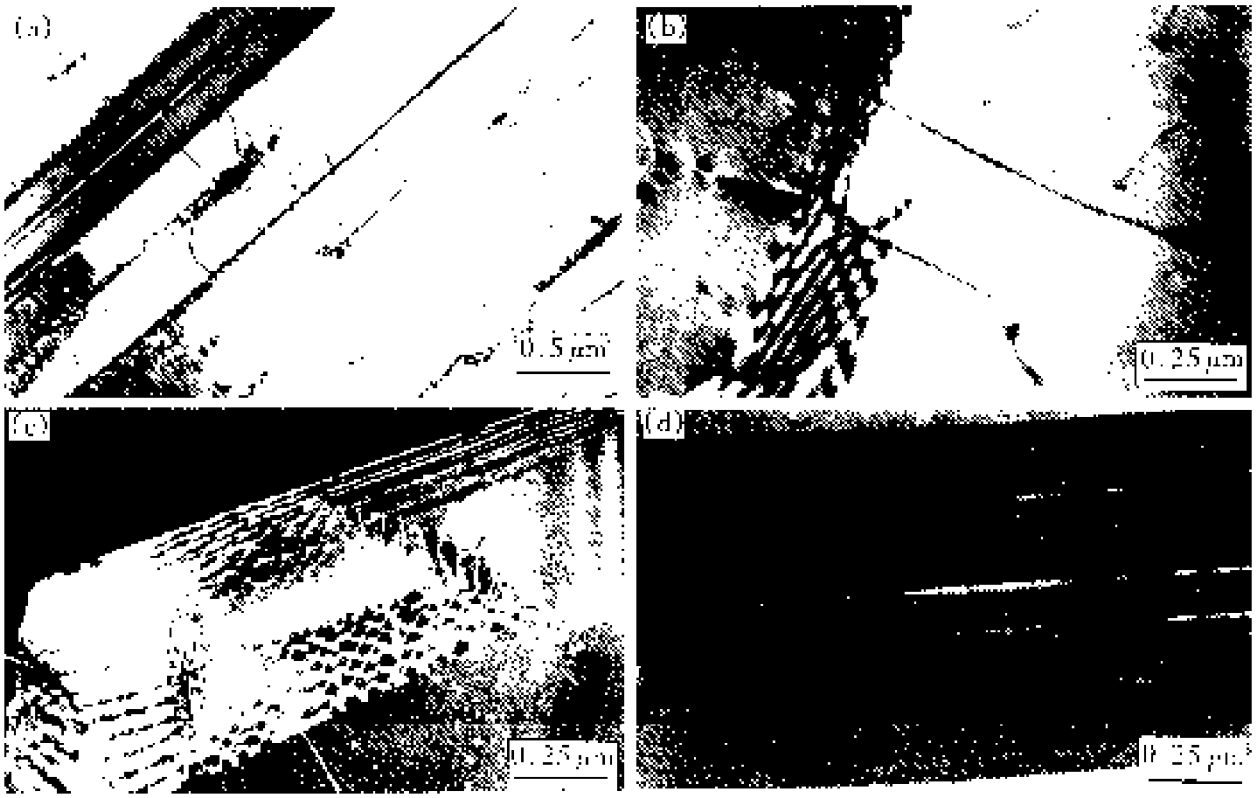

Fig. 4 Micrographs of deformed structure corresponding to secondary creep

(a) —the typical creep deformation structure in the samples with $\varphi = 45°$, $\sigma = 150$ MPa, $\varepsilon \approx 4\%$; (b) —dislocation wall in a γ plate; (c) —subgrain formed in a γ plate; (d) —twinning deformation in a γ plate

Table 2 The Schmid factors for the slip systems on (111) plane in γ domains with six orientations

planes	slip direction	variant I		variant II		variant III	
		matrix	twin	matrix	twin	matrix	twin
(111)	1/2[$1\bar{1}0$]	0	0	0.435	0.435	0.435	0.435
	[$01\bar{1}$]	0.435	0.435	0.435	0.435	0	0
	[$10\bar{1}$]	0.435	0.435	0	0	0.435	0.435
	1/6[$11\bar{2}$]	0.5	0.5	0.215	0.215	0.215	0.215

1/2[$1\bar{1}0$] dislocations are predicted to operate by the magnitude of the Schmid factor. So the magnitude of Schmid factors controls the activity of the slip or twinning system and results in the different deformation morphologies in γ plates with different variations.

Based on previous studies of creep deformation of γ-TiAl[4-6], the dependence of minimum creep rate on stress usually can be described using a power law description, in which creep deformation controlled by dislocation climb generally exhibits a stress exponent on the order of 4 to 5. Dislocation climb controlled creep also calls for an activation energy equal to that for self diffusion, given that creep is taking place within the high temperature regime of power law region. From the present results, the value of the stress exponent is 6.6, which is a little higher than that for dislocation climb controlled creep, but the creep activation energy of power law for the samples with $\varphi = 45°$ is 285 kJ/mol, which is close to that for Ti self diffusion and in agreement with the classical creep theory which predicts dislocation climb as rate limiting for creep. The observation to the deformation structure of the crept samples shows the formation of dislocation wall and substructure in some γ plates which results from dislocation climb. Based on these, we suggest that creep deformation of the sample with easy orientations within the present temperature and stress regime is primarily controlled by a dislocation climb process. But the higher stress exponent may be attribute to the character of lamellar structure in PST crystal. As discussed above, the deformation mechanism differs in the γ plates with different orientation variants, and in some γ plates, the twinning deformation occurs during creep, which can not be predicted by classical creep theory. It may be one of the reasons of high value of exponent for power law.

5 CONCLUSIONS

(1) The creep curves for PST crystals with easy orientation at 800 ℃, stress level range of 120 MPa to 200 MPa exhibit the steady state stage.

(2) The stress exponent and creep activation energy for power law are 6.6 and 285 kJ/mol respectively. With the observation to the creep deformation structure, we learn that the creep process is mainly controlled by the dislocation climb.

(3) The deformation structure observation by TEM shows that the deformation morphologies are different in each γ plates, which is attribute to the Schmid factors for slip or twinning system in γ plates with different orientation variants.

REFERENCES

1 Kim Y W. Acta Metal Mater, 1992, 40: 1121.
2 Takeyama. Mater Sci Eng, 1992, A152: 269.
3 Huang S C. In: Structural Intermetallics. Warrendale PA: The Minerals, Metals & Materials Society, 1993: 229.
4 Hayes R W, London B. Acta Metal Mater, 1992, 40: 2167.
5 Es-Souni M, Barrels, Wagner R. Mater Sci Eng, 1993, A171: 127.
6 Hiroshi, Oikawa. Mater Sci Eng, 1992, A153: 427.
7 Fujiwara T, Nakamura A and Yamaguchi. Philos Mag, 1990, A60: 591.
8 Swans R W *et al*. Creep in Metals and Alloys. London: The institute of Metals, 1985: 11.
9 Kroll S, Mehrer H *et al*. Mtallkd, 1992, 83: 8.

(Edited by He Xuefeng)